

Pyrethroid activity-based probes for profiling cytochrome P450 activities associated with insecticide interactions

Hanafy M. Ismail^{a,b}, Paul M. O'Neill^c, David W. Hong^c, Robert D. Finn^{d,e}, Colin J. Henderson^d, Aaron T. Wright^f, Benjamin F. Cravatt^g, Janet Hemingway^{a,1}, and Mark J. I. Paine^{a,1}

^aVector Biology, Liverpool School of Tropical Medicine, Liverpool L3 5QA, United Kingdom; ^bDepartment of Chemistry and Technology of Pesticides, Alexandria University, Alexandria, Egypt; ^cDepartment of Chemistry, University of Liverpool, Liverpool L69 7ZD, United Kingdom; ^dDivision of Cancer Research, Medical Research Institute, University of Dundee, Dundee DD1 9SY, United Kingdom; ^eDepartment of Applied Sciences, Northumbria University, Newcastle Upon Tyne NE1 8ST, United Kingdom; ^fBiological Sciences Division, Pacific Northwest National Laboratory, Richland, WA 99352; and ^gThe Skaggs Institute for Chemical Biology and Department of Chemical Physiology, The Scripps Research Institute, La Jolla, CA 92037

Contributed by Janet Hemingway, October 29, 2013 (sent for review August 27, 2013)

Pyrethroid insecticides are used to control diseases spread by arthropods. We have developed a suite of pyrethroid mimetic activity-based probes (PyABPs) to selectively label and identify P450s associated with pyrethroid metabolism. The probes were screened against pyrethroid-metabolizing and nonmetabolizing mosquito P450s, as well as rodent microsomes, to measure labeling specificity, plus cytochrome P450 oxidoreductase and *b*₅ knockout mouse livers to validate P450 activation and establish the role for *b*₅ in probe activation. Using PyABPs, we were able to profile active enzymes in rat liver microsomes and identify pyrethroid-metabolizing enzymes in the target tissue. These included P450s as well as related detoxification enzymes, notably UDP-glucuronosyltransferases, suggesting a network of associated pyrethroid-metabolizing enzymes, or “pyrethrome.” Considering the central role P450s play in metabolizing insecticides, we anticipate that PyABPs will aid in the identification and profiling of P450s associated with insecticide pharmacology in a wide range of species, improving understanding of P450–insecticide interactions and aiding the development of unique tools for disease control.

insecticide resistance | drug metabolism | interactome | malaria

Pyrethroids are synthetic analogs of pyrethrins, botanical chemicals derived from chrysanthemum flowers (1). They are highly potent insecticides with low mammalian toxicity that are used worldwide in ~3,500 registered products in agricultural, medicinal, veterinary, and public health sectors. Importantly, they are the only class of insecticide recommended for insecticide-treated nets for malaria control. More than 254 million insecticide-treated nets were distributed across Africa between 2008–2010 (2). Similar to antibiotics, pyrethroids are critical for controlling a diverse spectrum of diseases. Unfortunately, similar to antibiotics, such intense exposure affects health and drives the rapid evolution of insecticide resistance (3).

Pyrethroids are structurally highly diverse (4) but share a common architecture comprising a cyclopropane acid group coupled to an alcohol moiety, as exemplified by deltamethrin (Fig. 1A). Traditionally, they are divided into two classes (type 1 and type 2), depending on the absence (type 1) or presence (type 2) of an α -cyano group (Fig. 1B). Pyrethroids work by blocking the voltage-gated sodium channels, causing paralysis in arthropods, and resulting in death (3). Resistance is commonly associated with target site modification or metabolic resistance, in which increased rates of biotransformation, generally by P450s, esterases, and GSTs, reduce toxic potency (3).

Although the toxicity and metabolism of pyrethroids in mammals and insects have been extensively characterized (1), the role of specific enzymes and pathways involved in pyrethroid clearance is unclear. In insects, P450s are key enzymes involved with metabolic degradation, with constitutive overexpression of

specific P450s leading to pyrethroid resistance (5, 6). Similarly, in mammals, the toxic potency of pyrethroids is inversely related to their rates of metabolic elimination (7), with both P450 oxidation and carboxyl esterase-mediated hydrolysis playing major roles. Humans have 57 P450 genes, rodents ~80 P450 genes, and insects up to ~200 P450 genes (8). Where genome information exists, genetic and microarray-based studies of pyrethroid-resistant versus susceptible populations have been used to identify P450s potentially capable of pyrethroid metabolism (3, 5). However, relatively few P450s have been functionally validated through recombinant P450 expression. Thus, probes able to identify pyrethroid-metabolizing enzymes directly would aid our understanding of the fundamental processes of insecticide–organism interactions, expanding our understanding of the risks of pyrethroid exposure to mammals and the enzymatic mechanisms of metabolism and resistance used by insects.

Activity-based protein profiling (ABPP) has been described for the functional profiling of P450s (9, 10). The activity-based probes (ABPs) work in a mechanism-dependent manner to covalently label P450s, whereby the labeling events are detectable by adding a fluorescent reporter group via copper-catalyzed azide-alkyne cycloaddition (“click chemistry”) onto the probe–P450

Significance

Pyrethroids are highly potent insecticides used worldwide in ~3,500 registered products to control diseases spread by arthropods. Although they are critical for controlling a diverse spectrum of diseases, such intense exposure affects health and drives the rapid evolution of insecticide resistance. Here we have developed a suite of pyrethroid mimetic activity-based probes (PyABPs) to selectively label and identify P450s associated with pyrethroid metabolism in highly divergent organisms. Using a rat liver model, we demonstrate that PyABPs detect pyrethroid metabolizing P450s and a network of drug-metabolizing enzymes that is termed the “pyrethrome.” This discovery has broad scientific interest and provides a unique perspective on insecticide interactions, improving understanding of insecticide metabolism and aiding the development of tools for disease control.

Author contributions: H.M.I., P.M.O., J.H., and M.J.I.P. designed research; H.M.I. performed research; D.W.H., R.D.F., C.J.H., A.T.W., and B.F.C. contributed new reagents/analytic tools; H.M.I., P.M.O., D.W.H., J.H., and M.J.I.P. analyzed data; and H.M.I. and M.J.I.P. wrote the paper.

The authors declare no conflict of interest.

Freely available online through the PNAS open access option.

¹To whom correspondence may be addressed. E-mail: M.J.Paine@liverpool.ac.uk or hemingway@liverpool.ac.uk.

This article contains supporting information online at www.pnas.org/lookup/suppl/doi:10.1073/pnas.1320185110/-DCSupplemental.

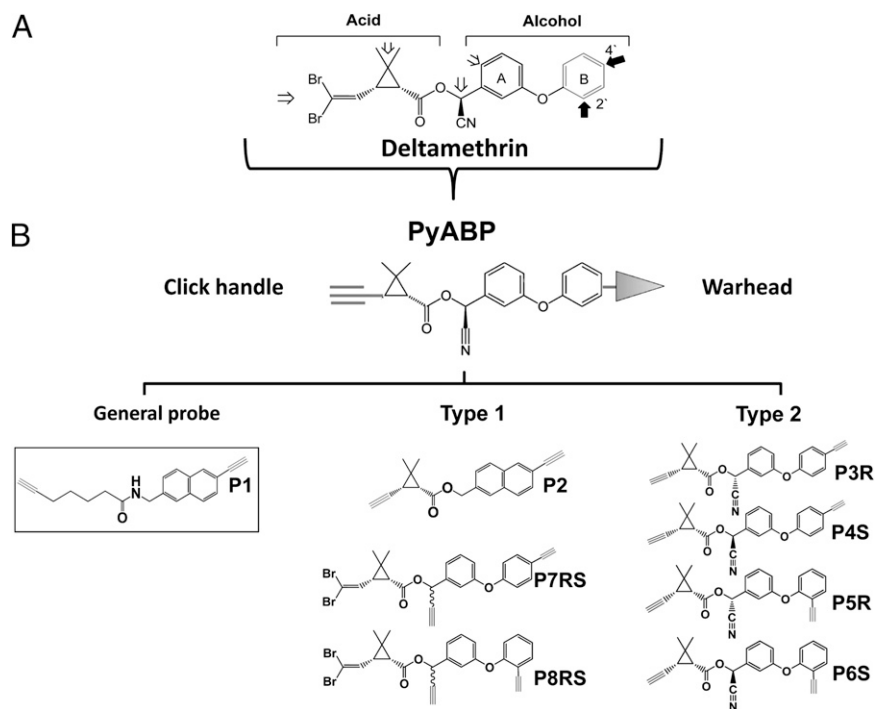


Fig. 1. Conversion of deltamethrin into PyABPs. (*A*) Structure of deltamethrin with constituent acid and alcohol moieties. Primary sites of P450 hydroxylation are indicated by bold arrows at the 2' and 4' positions, and minor routes of hydroxylation are indicated with open arrows (1). (*B*) Conversion of deltamethrin to a PyABP involves the addition of an alkyne warhead and a clickable handle. The structures of the general probe and the PyABPs synthesized are illustrated. Alkyne warhead groups were located in the 2' or 4' positions, whereas alkyne click handles replaced the cyano group (type 1) or terminal bromides (type 2). The general P450 probe 2-EN is boxed parallel to its type 1 pyrethroid analog, P2.

adducts (9, 10). Furthermore, affinity tags can also be incorporated to pull down and identify probe–P450 adducts. The major advantage of ABPPs is their ability to directly assess enzyme activity. In this article, we have designed and synthesized a group of seven pyrethroid mimetic ABPs (PyABPs) on the basis of the deltamethrin scaffold (Fig. 1*B*) for the targeted identification of pyrethroid-metabolizing P450s in highly divergent organisms. We have investigated their reactivity profiles against pyrethroid-metabolizing and nonmetabolizing recombinant mosquito P450s and mouse and rat liver microsomes. We show that PyABPs can be used to reveal pyrethroid structure–activity relationships, and they also have been used to identify pyrethroid-reactive P450s and related detoxification enzymes in rat liver microsomes, demonstrating their potential for directly assessing pyrethroid-metabolizing enzyme activity.

Results and Discussion

Design and Synthesis of PyABPs. To function, P450-ABPs must contain a reactive alkyne warhead for P450 inactivation and covalent attachment, as well as an acetylene moiety for click-chemistry-mediated addition of reporter groups or affinity tags (Fig. 1*B*). Thus, a suite of seven PyABPs were synthesized, varying in the positioning of warhead and click-handles, to investigate structure–activity relationships and optimize probe reactivity (Fig. 1*A*; *SI Appendix*). The probes were designated as P2, P3R, P4S, P5R, P6S, P7RS, and P8RS.

All PyABPs apart from P2 were synthesized using a deltamethrin scaffold. P2 was based on a 2-ethynyl-1-naphthalenol (Probe 1) scaffold, a P450 ABPP with a broad spectrum of activity (9). The reactive alkyne groups (warheads) were located on the phenoxybenzyl alcohol group in the 2' or 4' positions to promote catalysis and mechanism-based inactivation (Fig. 1*B*), the predominant sites of P450 oxidation of deltamethrin (11, 12). The click-handle for fluorescent reporter and/or affinity purification tag

attachment was placed terminally, replacing the bromide atoms on the cyclopropane group to produce type 2 pyrethroids P3R, P4S, P5R, and P6S, or in the middle, replacing the α -cyano group on the central alpha carbon to produce type 1 pyrethroids P7RS and P8RS.

Because the specificity and rate of metabolic detoxification are dependent on the isomeric state and presence of the α -cyano substituent, as well as the composition and flexibility of the phenoxybenzyl group (4), the suite of probes was designed to allow us to address the positioning effects of the warhead and click-handles, as well as isomer effects and structural flexibility (Fig. 1*B*). As a consequence, type 1 (nonyano) PyABPs P7RS and P8RS were paired isomer mixtures (R/S; 1:1), differing only in the positioning of the warhead (4' and 2', respectively). Type 2 PyABPs P3R and P4S were pure R and S isomers with a 4' warhead, whereas P5R and P6S were, respectively, R and S isomers containing a 2' warhead. Finally, P2 allowed us to examine the effect of a rigid planar biphenyl group in place of a flexible aromatic group on PyABP activity.

Labeling Pyrethroid-Metabolizing P450s and Interrogating Structure–Activity Relationships. To test their capacity to label P450s, the PyABPs were screened against two recombinant mosquito P450s, cytochrome P450 6M2 (CYP6M2) and cytochrome P450 6Z2 (CYP6Z2). These P450s are strongly associated with pyrethroid resistance in the malaria-transmitting species *Anopheles gambiae*, but with contrasting abilities to metabolize deltamethrin (11, 13, 14); deltamethrin is metabolized by CYP6M2 but not CYP6Z2 (15). Probes were added to *Escherichia coli* membranes coexpressing recombinant P450 and its obligate redox partner *An. gambiae* NADPH cytochrome P450 oxidoreductase (CPR), in the presence or absence of NADPH, to confirm that P450 labeling occurred in an activity-dependent manner. After incubation, membranes were treated with an azide-conjugated

Alexa Fluor 488 fluorescent tag under click-chemistry conditions, resolved by SDS/PAGE, and P450 labeling identified by in-gel fluorescence scanning (Fig. 2A). Background (–NADPH) probe reactivity is commonly observed with ABPs when screening recombinant P450s (9) and is likely a result of the high P450 content and residual probe binding. Heat maps were therefore generated by subtraction of –NADPH signals to provide a more quantitative assessment of probe activity (Fig. 2B).

As expected, the probe-labeling profiles of the two P450s were quite different (Fig. 2), broadly reflecting their known capacities for pyrethroid metabolism (15–17). CYP6M2 reacted strongly with both P7RS and P8RS but displayed weak activity with the remaining pyrethroid probes and no activity with P1. In contrast, CYP6Z2 showed strong reactivity with P1 but weak or no activity against the PyABPs, apart from P8RS. This provided insight into their structure–activity relationships. For example, both the dibromo-vinyl-containing probes P7RS and P8RS were highly reactive with CYP6M2, despite different warhead positions (2' and 4', respectively), in contrast to the less-reactive type 2 probes with the terminal click-handle replacement (Fig. 2). This suggests an influential role for the dibromo-vinyl group in PyABP docking and metabolism. In contrast, loss of the α -cyano group appeared to have minimal effect on metabolism, which is supported by the fact that the noncyano pyrethroid permethrin and the cyano pyrethroid deltamethrin have similar rates of metabolism by CYP6M2 (11). Overall, these results suggest that placement of the acetylene handle at the C α position provides the best probe mimetic of deltamethrin.

Metabolism by CYP6M2 was unaffected by the 2' or 4' positioning of the acetylene groups. This is likely a result of the flexibility of the biphenyl group allowing productive heme–ligand poses in both warhead positions. Intriguingly, although considered a nonmetabolizer, CYP6Z2 was highly reactive with P8RS, indicating that pyrethroid metabolism is possible but structurally constrained to the 2' position of the phenoxybenzyl region. This fits the highly selective substrate profile of this P450, which can accommodate smaller molecules such as phenoxybenzyl pyrethroid metabolites 3-phenoxybenzyl alcohol and 3-phenoxybenzaldehyde carbaryl and resveratrol, but not larger molecules such as dichlorodiphenyltrichloroethane and alpha cypermethrin (16). With respect to isomer effects, in general, the S form of an α -cyano pyrethroid isomer is more toxic than the R isomer (1). The effect of the cis versus trans pairings P3R versus P4S and

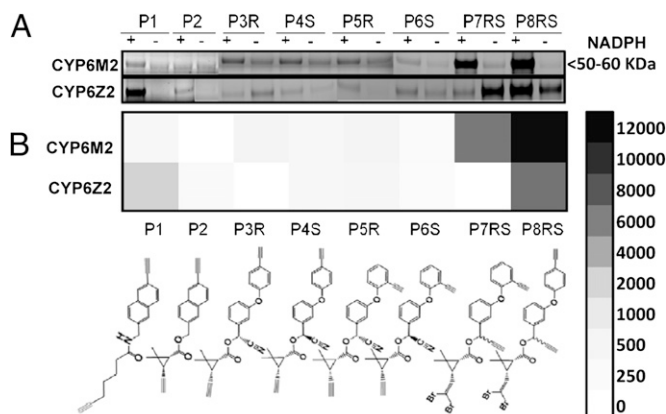


Fig. 2. PyABP profiling with pyrethroid-metabolizing (CYP6M2) and non-metabolizing (CYP6Z2) mosquito P450s. (A) Fluorescent gel; 50–60-kDa region of SDS/PAGE separation of *E. coli* membranes expressing recombinant P450. (B) Heat maps, with probe structures below, illustrating probe-labeling profiles corresponding to the fluorescent gel lanes; heat signals were normalized by subtraction of –NADPH from +NADPH signals. Fluorescence intensity values are given in arbitrary units.

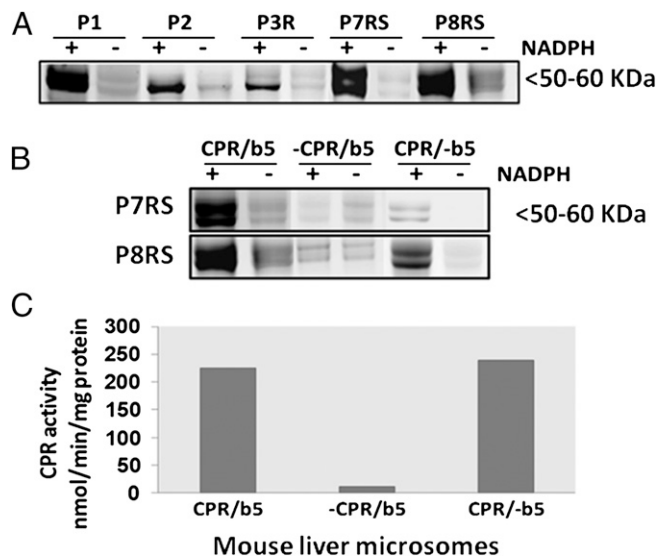


Fig. 3. Probe labeling of mouse and mosquito microsomes. (A) Treatment of mouse liver microsomal proteome with P1 and a selection of PyABPs. (B) Labeling of mouse liver microsomal proteomes from normal (CPR/ b_5), CPR knockout (–CPR/ b_5), and b_5 knockout (CPR/– b_5) animals with P7RS and P8RS. (C) CPR activity in mouse liver microsomes.

P5R versus P6S on probe reactivities was inconclusive, as the probe reactivities were weak.

Probing Redox Partner Interactions in Mouse Liver Microsomes. To examine the ability of PyABPs to label P450s in a complex proteome, P7RS, along with P1, P2, P3R, and P8RS, were tested against mouse liver microsomes in the presence or absence of NADPH (Fig. 3A). Fluorescent signals in the 50–60-kDa region were observed in the presence of NADPH, consistent with P450 labeling (9). P7RS produced the strongest signal, along with P1. P8RS also produced a strong signal, although the sample had significantly less signal difference between –NADPH and +NADPH; minor labeling occurred in most lanes, either as a result of residual NADPH in the microsomes or, more likely, as a reflection of high-affinity probe binding. P7RS and P8RS were also incubated with mouse membranes lacking CPR (18) or cytochrome b_5 (b_5) (19, 20) to gain insight into the role of P450 redox partners in PyABP metabolism (Fig. 3B). Being the obligate redox partner for P450s, probes were not expected to be active in CPR knockout mice. The role of b_5 , in contrast, is unclear (11). Previous analysis on individual human P450s has shown that b_5 can stimulate, inhibit, or have no effect on P450-mediated reactions, depending on the experimental conditions and substrates analyzed (21, 22), and that it can alter the types of metabolites produced from a single substrate (23). However, these data are confounded by the fact that much of the literature is based on in vitro assays of isolated components. Given that the activity of many recombinant mosquito P450s that metabolize pyrethroids are augmented by b_5 (11, 16), we were keen to investigate the influence of b_5 on pyrethroid metabolism in a more natural context. As expected, labeling was greatly reduced in the CPR knockout microsomes compared with the normal mouse liver (Fig. 3B), consistent with a lack of CPR activity (Fig. 3C). However, both P7RS and P8RS labeled proteins in the 50–60-kDa size range in b_5 knockout mice (CPR/– b_5 ; Fig. 3B), but with much weaker signal strength. These differences indicate that the effects of b_5 are substrate-dependent. In conclusion, these results demonstrate that b_5 can modulate pyrethroid metabolism in the liver microsomes, providing unique insight into pyrethroid–P450– b_5 interactions.

Identification of the P7RS Interactome (Pyrethrome) in Rat Liver. To investigate the ability of PyABPs to directly identify pyrethroid-metabolizing enzymes in native tissue, P7RS labeling of rodent liver microsomes was performed. Because of the widespread use of this subcellular fraction for drug metabolism studies, P450 enzymes therein are well-characterized (7). P7RS produced a strong NADPH-dependent fluorescent signal in the 50–60-kDa region after labeling and affinity purification with a multimodal reporter, rhodamine–biotin azide (9) (Fig. 4A). After SDS/PAGE separation, the strongly labeled banding region, between 50 and 60 kDa, was excised and subjected to in-gel trypsin digestion, and the resulting peptides were analyzed by liquid chromatography tandem mass spectrometry (LC-MS/MS). Proteins were identified using the Mascot search algorithm and semiquantified by the exponentially modified protein abundance index (emPAI), based on protein coverage by the peptide matches in a database search, allowing approximate, label-free, relative quantitation of proteins in a mixture (24). Enzymes that catalyze the biotransformation of drugs and xenobiotics are generally classified into two main groups: phase 1 oxidative enzymes such as P450s and phase 2 conjugative enzymes such as UDP-glucuronosyltransferases (UGTs) and glutathione S transferases. As expected, most of the enzymes isolated were P450s (84%, emPAI) (Fig. 4B; *SI Appendix, Table S1*), of which CYP2C11 and CYP2C6 were the two most abundant targets [46% and 19% (emPAI), respectively; *SI Appendix, Table S1*]. Importantly, both CYP2C11 and CYP2C6 exhibit high rates of deltamethrin metabolism (K_M , 32 μM , and V_{max} , 206 min^{-1} ; and K_M , 22 μM , and V_{max} , 150 min^{-1} , respectively) (7), demonstrating the probes' ability to target deltamethrin metabolizers. Results were also consistent with known high levels of expression of CYP2C11 and CYP2C6 in rat livers (7) and with confirmation of a major role for these P450s in the oxidative metabolism of deltamethrin in rats. Two of the other most abundant P450s pulled-down by P7RS, CYP2C13 and CYP2D1 (*SI Appendix, Table S1*), are known to metabolize pyrethroids (7, 12, 25), reiterating the probe's ability to identify pyrethroid-metabolizing P450s. CYP3A2, a highly expressed P450 in rat liver that metabolizes pyrethroids (7), was notably present in the low-abundance fraction (1%). This is consistent with a lower rate of deltamethrin metabolism and a minor role in deltamethrin metabolism in rat liver (7) and suggests that

biologically relevant probe interactions extend to the low-abundance enzyme fraction.

For further validation, experiments were repeated using a slightly different approach. Here, P7RS-bound proteins were affinity-purified on streptavidin beads, using a biotin-azide reporter, followed by on-bead trypsin digestion instead of gel-band excision. LC/MS of resultant peptides identified a similar set of enzymes, with CYP2C11 as the top hit followed by CYP2D10 and CYP2D1 (*SI Appendix, Table S2*). CYP2D1 metabolizes α -cypermethrin, λ -cyhalothrin, and β -cyfluthrin (12), which are pyrethroids that are structurally similar to deltamethrin. It also shares high-amino-acid identity with CYP2D10 (96%) and the other members of the CYP2D family that were pulled-down (*SI Appendix, Tables S1 and S2*). Percentage identities were as follows: CYP2D3 (79% identity), CYP2D26 (73%), CYP2D4 (72%), and CYP2D18 (72%), suggesting a common ability to metabolize pyrethroids. Although similar sets of enzymes were identified by in-gel and on-bead trypsin digestion, there were notable differences in their rank order. This likely reflects differences in sensitivities of the two approaches, as well as differences in microsome preparations.

It was also evident that several enzymes other than P450s also reacted with P7RS. Interestingly, all were drug-metabolizing enzymes, suggesting functional rather than nonspecific probe interactions, consistent with the fact that ABPs are reported to capture functional pathways (26). This may occur through protein–protein interactions or by transient diffusion of a reactive probe intermediate out of the active site of a P450, followed by reaction with a protein in close proximity to the P450 (9, 27).

Overall, P7RS interactions with rat liver microsomes suggest a network of drug-metabolizing enzymes associated with pyrethroid metabolism, or “pyrethrome.” There is accruing evidence that orchestrated interactions between P450s and UGTs, which lie opposite P450s on the luminal side of the endoplasmic reticulum, may facilitate the channeling and excretion of toxic and reactive intermediate metabolites (28–30). This is supported here by the interactions of UDP-glucuronosyltransferases 2B2, 2B3, 2B4 and 2B5 (UDP-g 2Bs 2–5) with P7RS (Fig. 4 and *SI Appendix, Tables S1 and S2*). Indeed, glucuronide conjugation of permethrin ester hydrolysis products has been demonstrated in rats (31), and thus, such compounds could form protein–pyrethroid

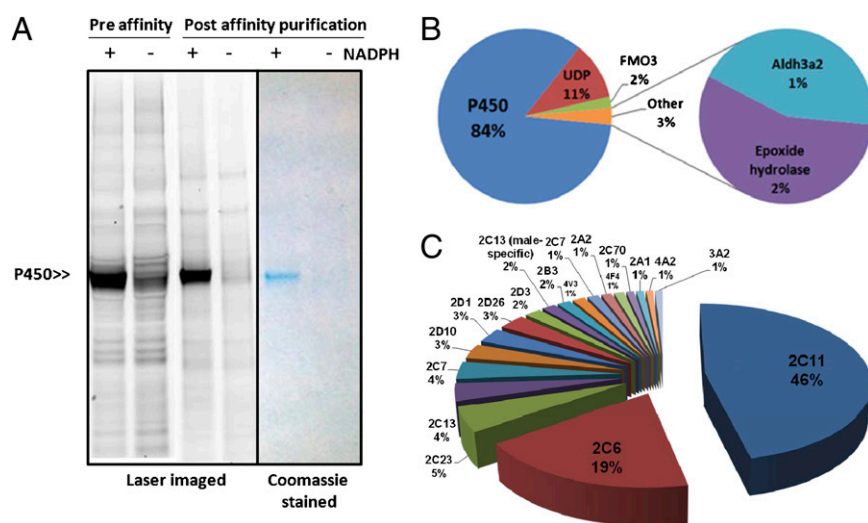


Fig. 4. Proteins identified in a rat liver microsomal proteome by P7RS and in-gel LC-MS/MS. (A) P7RS targets were detected after labeling by click chemistry (preaffinity lanes) and affinity purification (postaffinity lanes) with a rhodamine–biotin azide tag by SDS/PAGE and in-gel fluorescence. The enriched affinity purified P450 band (~50–60 kDa) visible by Coomassie staining was excised for LC-MS/MS proteomic analysis. (B) Percentage constitution of detoxification enzymes labeled by P7RS. (C) Percentage constitution of individual P450s identified. Percentage constitutions were calculated on the basis of emPAI for each protein relative to the total emPAI, as indicated in *Methods*.

conjugates on transacylation or via Amadori product formation (31). Flavin-containing monooxygenase 3 (2%, emPAI), which catalyzes the NADPH-dependent oxygenation of various nitrogen-, sulfur-, and phosphorus-containing xenobiotics, and ALDH3a2, which is responsible for the oxidation of aldehyde to carboxylic acids, were also present (Fig. 3). Whether close contact interactions occur with P450s and/or UGTs in connection with a coordinated pyrethrome-mediated metabolism of pyrethroids has yet to be established.

Conclusions

Here, we have synthesized and tested a unique panel of ABPs and PyABPs directed toward pyrethroid-metabolizing P450s. Screening of the probes against recombinant mosquito P450s identified optimal probes for P450s that metabolized pyrethroid substrates. One such probe, P7RS, was taken forward to establish its capabilities as a deltamethrin mimic probe. We have demonstrated that P7RS was capable of detecting deltamethrin-metabolizing P450s in a complex rat proteome, as well as UGT and other enzymes associated with xenobiotic metabolism. These may simply reflect individual, but unrelated, probe interactions. However, our favored interpretation is that the probe has captured a pyrethrome, an associated network of enzymes involved in pyrethroid metabolism. Regardless, the power of the PyABP to directly assess pyrethroid metabolizing activity is significant. Considering the central role that P450s play in insecticide metabolism, we anticipate that PyABPs will prove of value for assessing P450–pyrethroid interactions in a wide range of species and biological systems, and in tropical diseases in particular. For instance, in 2012, largely in response to escalating pyrethroid resistance, the World Health Organization launched an international call to action with its Global Plan for Insecticide Resistance Management for Malaria Vectors (32). The probes described here could be used to profile P450s associated with pyrethroid resistance in a wide spread of mosquito vectors, to characterize mechanisms of resistance and identify potential resistance markers. Similarly, they would be of value for profiling metabolic resistance in veterinary and agricultural pests, where pyrethroids are used extensively. Finally, ABPs are versatile in probing drug interactions in vivo (9, 10). Given that the pharmacology of insecticide metabolism is poorly understood in relation to drug metabolism, PyABPs may be used in the future to facilitate the functional characterization of insecticide activity in vivo.

Methods

Chemicals and Reagents. β -Nicotinamide adenine dinucleotide phosphate, reduced form, tetrasodium salt (NADPH) was obtained from Melford. Luminescent P450 activity assays were performed in white 96-well plates (Thermo Fisher Scientific), using the commercially available P450-Glo's substrate Luciferin-PPXE (Promega). DMSO solvents were reagent-grade (Sigma Aldrich). The click-chemistry ligand, Tris [(1-benzyl-1H-1, 2, 3-triazol-4-yl) methyl] amine, was purchased from Sigma-Aldrich Chemical Co. Alexa Fluor 488 azide and biotin azide were purchased from Invitrogen. The chemical synthesis of the probes (PyABPs) is described in *SI Appendix*.

Preparation of Membranes Expressing P450s. *E. coli* membranes coexpressing CYP6M2 or CYP6Z2 with CPR were prepared as previously described (11, 15). Rat liver microsomes were prepared from male Wistar rats kindly provided by Alison Shone (Molecular Biochemical Parasitology group, Liverpool School of Tropical Medicine, Liverpool, United Kingdom).

Male mouse liver microsomes samples, kindly provided by Roland Wolf (Biomedical Research Institute, University of Dundee, United Kingdom), were prepared from transgenic animals that have conditional deletions of liver CPR or b_5 along with normal mouse controls, as described (20, 33).

Probe Labeling of Pyrethroid-Metabolizing P450s. Recombinant P450s CYP6M2 and CYP6Z2 were normalized to 0.2 μ M in Ca^{2+} and Mg^{2+} free Dulbecco's Phosphate Buffer Saline (D-PBS; Invitrogen) at pH 7.4 and treated with probes at 20 μ M in the presence and absence of 1 mM NADPH. All probes were prepared as 20-mM stock solutions in DMSO. Samples were incubated

at 37 °C for 1 h. Thereafter, 44 μ L of sample was transferred to an Eppendorf tube for addition of 0.5 μ L Alexa Fluor 488 azide reporter (5 mM stock solution in DMSO). After addition of the reporter, the click chemistry reaction proceeded with conditions optimized by Speers and Cravatt (34). Briefly, samples were treated with 1 μ L Alexa Fluor 488 azide reporter (2.5 mM stock in DMSO), followed by 1 μ L freshly prepared Tris(2-carboxyethyl)phosphine hydrochloride (50 mM stock in water) and 3.3 μ L ligand (1.7 mM stock in DMSO:t-butanol 1:4), giving a t-butanol concentration of 5% (vol/vol). Samples were gently vortexed, and 1 μ L CuSO_4 (50 mM stock in water) was added. Each sample was gently vortexed and allowed to react at room temperature for 1 h in the dark, with regular vortexing every 15 min. NuPAGE Novex 4–12% Bis-Tris Gels (Invitrogen) were used for protein separation, whereby 2 \times SDS/PAGE loading buffer (reducing) was added to each reaction, the samples were heated at 90 °C for 8 min, and then 30 μ L per well were loaded onto gels. Gels were destained (5:4:1 water/methanol/acetic acid) overnight in the dark, and fluorescence intensities were measured using an Ettan DIGE Laser imager (GE Healthcare) with a CY2 filter. Equal protein loading was confirmed by post scanstaining with Gel code Blue Coomassie stain (Pierce).

Probe Labeling of Rodent Microsomes. Rat liver microsomes were normalized to 2 mg/mL protein and treated with 20 μ M PyABPs in the presence and absence of 1 mM NADPH. For mouse liver microsomes, the P450 contents were adjusted to 0.2 μ M and treated with 20 μ M PyABPs in the presence and absence of 1 mM NADPH. Samples were incubated at 37 °C for 1 h and then labeled proteins were identified by gel fluorescence scanning, after appending AlexaFluor488-azide at 25 μ M to labeled proteome via click-chemistry, as described earlier.

Identification of P7RS Metabolizing Enzymes in Rat Liver Microsomes. One microliter rat liver microsomes (2 mg/mL protein in PBS) was treated with 2.0 μ L probe P7RS (10 mM stock solution in DMSO) in the presence or absence of 1 mM NADPH. The samples were incubated at 37 °C for 45 min and then treated with a multimodal biotin–rhodamine azide reporter group for in-gel detection or a biotin–azide reporter for on-bead trypsin digestin (both 4.0 μ L of a 5 mM stock solution in DMSO), followed by vortexing. The click reaction was preceded by addition of click-chemistry reagents, as previously described, and left at room temperature in the dark for 1 h. Rhodamine–biotin azide tag-labeled proteins were enriched with streptavidin agarose beads, as previously mentioned (9). Briefly, samples were centrifuged (5,900 $\times g$, 4 min, 4 °C) to pellet the protein. The supernatant was discarded, cold methanol (0.40 mL) was added to the pellets, and the proteins were resuspended by sonication (3–5 s) and then rotated (10 min, 4 °C). The centrifugation step was repeated, the supernatant was discarded, methanol (0.40 mL) was added to the pellets, and the proteins were resuspended by sonication (3–5 s) and then rotated (10 min, 4 °C) once again. The samples were pelleted by centrifugation once more, and the supernatant discarded. PBS (1.0 mL) containing SDS (1.2%, vol/vol) was added to the pellets and subsequently resuspended by sonication (3–5 s). The samples were heated at 90 °C for 8 min and then cooled to room temperature. Proteins were then enriched by rotating samples (1.5 h) with streptavidin-agarose beads (0.1 mL suspension solution) in a PBS media diluted to 0.2% SDS. The PBS media was removed, and the beads were rinsed with 0.2% SDS in PBS (1.5 mL, 3 \times), urea (6.0 M, 1.5 mL, 3 \times), and PBS buffer (1.5 mL, 3 \times).

For in-gel detection, SDS/PAGE loading buffer (2 \times , reducing, 50 μ L) was added to the beads and heated at 90 °C for 8 min. The samples (35 μ L) were loaded onto SDS/PAGE gels and separated. Gels were imaged onto Ettan DIGE Laser imager (GE Healthcare) at CY3 filter to determine the labeling in presence and absence of NADPH. After imaging, the gel Coomassie stained, using Gel code Blue Coomassie stain (Pierce). The darkly stained bands from 48 to 55 kDa were excised with a razor blade and diced into small cubes. The gel pieces were washed with water and sent to Dundee University (<http://proteomics.lifesci.dundee.ac.uk/service-rates>) for trypsin digestion and LC-MS/MS analysis.

For on-bead trypsin digestion, probe-labeled proteins were enriched and identified after the click reaction incubation reaction, using streptavidin agarose beads, as described previously (35).

Proteins were identified using the Mascot search algorithm and semiquantified by the emPAI (24). This value offers approximate, label-free, relative quantitation of proteins in a mixture. This is obtained on the basis of protein coverage by the peptide matches in a database search. Data were filtered on the ions score, which is calculated using $-\text{Log}(P)$, where P is the probability that the observed match is a random event. Individual ions scores >41 indicate identity or extensive homology ($P < 0.05$). Protein scores were derived from ion scores on a nonprobabilistic basis for ranking protein hits.

ACKNOWLEDGMENTS. The authors were funded by the Innovative Vector Control Consortium (M.J.I.P., H.M.I., J.H.), the William Hesketh Leverhulme foundation (H.M.I.), a Cancer Research UK programme grant

(C4639/A12330 to C.J.H. and R.D.F.) and National Institutes of Health CA87660 (to B.F.C. and A.T.W.), GM103493 (to A.T.W.) and CA087660 (to B.F.C.).

1. Khambay BPS, Jewess PJ (2004) Pyrethroids. *Comprehensive Molecular Insect Science*, eds Gilbert LI, Iatrou K, Gill SS (Pergamon Press, Oxford), Vol 6, pp 1–29.
2. WHO (2010) *World Malaria Report* (World Health Organization, Geneva, Switzerland).
3. Ranson H, et al. (2011) Pyrethroid resistance in African anopheline mosquitoes: What are the implications for malaria control? *Trends Parasitol* 27(2):91–98.
4. Casida JE, Gammon DW, Glickman AH, Lawrence LJ (1983) Mechanisms of selective action of pyrethroid insecticides. *Annu Rev Pharmacol Toxicol* 23:413–438.
5. David JP, Ismail HM, Chandor-Proust A, Paine MJ (2013) Role of cytochrome P450s in insecticide resistance: Impact on the control of mosquito-borne diseases and use of insecticides on Earth. *Philos Trans R Soc Lond B Biol Sci* 368(1612):20120429.
6. Li X, Schuler MA, Berenbaum MR (2007) Molecular mechanisms of metabolic resistance to synthetic and natural xenobiotics. *Annu Rev Entomol* 52:231–253.
7. Godin SJ, et al. (2007) Identification of rat and human cytochrome p450 isoforms and a rat serum esterase that metabolize the pyrethroid insecticides deltamethrin and esfenvalerate. *Drug Metab Dispos* 35(9):1664–1671.
8. Nelson DR (2009) The cytochrome p450 homepage. *Hum Genomics* 4(1):59–65.
9. Wright AT, Cravatt BF (2007) Chemical proteomic probes for profiling cytochrome p450 activities and drug interactions in vivo. *Chem Biol* 14(9):1043–1051.
10. Wright AT, Song JD, Cravatt BF (2009) A suite of activity-based probes for human cytochrome P450 enzymes. *J Am Chem Soc* 131(30):10692–10700.
11. Stevenson BJ, et al. (2011) Cytochrome P450 6M2 from the malaria vector *Anopheles gambiae* metabolizes pyrethroids: Sequential metabolism of deltamethrin revealed. *Insect Biochem Mol Biol* 41(7):492–502.
12. Scollon EJ, Starr JM, Godin SJ, DeVito MJ, Hughes MF (2009) In vitro metabolism of pyrethroid pesticides by rat and human hepatic microsomes and cytochrome p450 isoforms. *Drug Metab Dispos* 37(1):221–228.
13. Djouaka RF, et al. (2008) Expression of the cytochrome P450s, CYP6P3 and CYP6M2 are significantly elevated in multiple pyrethroid resistant populations of *Anopheles gambiae* s.s. from Southern Benin and Nigeria. *BMC Genomics* 9:538.
14. Müller P, et al. (2008) Pyrethroid tolerance is associated with elevated expression of antioxidants and agricultural practice in *Anopheles arabiensis* sampled from an area of cotton fields in Northern Cameroon. *Mol Ecol* 17(4):1145–1155.
15. McLaughlin LA, et al. (2008) Characterization of inhibitors and substrates of *Anopheles gambiae* CYP6Z2. *Insect Mol Biol* 17(2):125–135.
16. Chiu TL, Wen Z, Rupasinghe SG, Schuler MA (2008) Comparative molecular modeling of *Anopheles gambiae* CYP6Z1, a mosquito P450 capable of metabolizing DDT. *Proc Natl Acad Sci USA* 105(26):8855–8860.
17. Chandor-Proust A, et al. (2013) The central role of mosquito cytochrome P450 CYP6Zs in insecticide detoxification revealed by functional expression and structural modelling. *Biochem J* 455(1):75–85.
18. Henderson CJ, et al. (2003) Inactivation of the hepatic cytochrome P450 system by conditional deletion of hepatic cytochrome P450 reductase. *J Biol Chem* 278(15):13480–13486.
19. McLaughlin LA, Ronseaux S, Finn RD, Henderson CJ, Roland Wolf C (2010) Deletion of microsomal cytochrome *b*₅ profoundly affects hepatic and extrahepatic drug metabolism. *Mol Pharmacol* 78(2):269–278.
20. Finn RD, et al. (2008) Defining the in Vivo Role for cytochrome *b*₅ in cytochrome P450 function through the conditional hepatic deletion of microsomal cytochrome *b*₅. *J Biol Chem* 283(46):31385–31393.
21. Paine MJ, Scrutton NS, Munro AW, Roberts GCK, Wolf CR (2004) Electron Transfer Partners of Cytochrome P450. *Cytochromes P450: Structure, Mechanism and Biochemistry*, ed Ortiz de Montellano PR (Kluwer Academic/Plenum Publishers, New York), 3rd Ed, pp 115–148.
22. Schenkman JB, Jansson I (1999) Interactions between cytochrome P450 and cytochrome *b*₅. *Drug Metab Rev* 31(2):351–364.
23. Kotrbová V, et al. (2011) Cytochrome *b*(5) shifts oxidation of the anticancer drug ellipticine by cytochromes P450 1A1 and 1A2 from its detoxication to activation, thereby modulating its pharmacological efficacy. *Biochem Pharmacol* 82(6):669–680.
24. Ishihama Y, et al. (2005) Exponentially modified protein abundance index (emPAI) for estimation of absolute protein amount in proteomics by the number of sequenced peptides per protein. *Mol Cell Proteomics* 4(9):1265–1272.
25. Stresser DM, Turner SD, Blanchard AP, Miller VP, Crespi CL (2002) Cytochrome P450 fluorometric substrates: Identification of isoform-selective probes for rat CYP2D2 and human CYP3A4. *Drug Metab Dispos* 30(7):845–852.
26. Wiedner SD, et al. (2012) Multiplexed activity-based protein profiling of the human pathogen *Aspergillus fumigatus* reveals large functional changes upon exposure to human serum. *J Biol Chem* 287(40):33447–33459.
27. Cravatt BF, Wright AT, Kozarich JW (2008) Activity-based protein profiling: From enzyme chemistry to proteomic chemistry. *Annu Rev Biochem* 77:383–414.
28. Ishii Y, Takeda S, Yamada H (2010) Modulation of UDP-glucuronosyltransferase activity by protein-protein association. *Drug Metab Rev* 42(1):145–158.
29. Jensen NB, et al. (2011) Convergent evolution in biosynthesis of cyanogenic defence compounds in plants and insects. *Nat Commun* 2:273, 10.1038/ncomms1271.
30. Radomska-Pandya A, Bratton SM, Redinbo MR, Miley MJ (2010) The crystal structure of human UDP-glucuronosyltransferase 2B7 C-terminal end is the first mammalian UGT target to be revealed: The significance for human UGTs from both the 1A and 2B families. *Drug Metab Rev* 42(1):133–144.
31. Noort D, van Zuylen A, Fidder A, van Ommen B, Hulst AG (2008) Protein adduct formation by glucuronide metabolites of permethrin. *Chem Res Toxicol* 21(7):1396–1406.
32. WHO (2012) *Global Plan for Insecticide Resistance Management (GPIRM)* (World Health Organization, Geneva, Switzerland).
33. Finn RD, et al. (2011) Cytochrome *b*₅ null mouse: A new model for studying inherited skin disorders and the role of unsaturated fatty acids in normal homeostasis. *Transgenic Res* 20(3):491–502.
34. Speers AE, Cravatt BF (2004) Profiling enzyme activities in vivo using click chemistry methods. *Chem Biol* 11(4):535–546.
35. Speers AE, Cravatt BF (2009) Activity-Based Protein Profiling (ABPP) and Click Chemistry (CC)-ABPP by MudPIT Mass Spectrometry. *Curr Protoc Chem Biol* 1:29–41.